Cellular/Molecular

Presynaptic Serotonergic Gating of the Subthalamonigral Glutamatergic Projection

Shengyuan Ding, Li Li, and Fu-Ming Zhou
Department of Pharmacology, University of Tennessee College of Medicine, Memphis, Tennessee 38163

The GABAergic projection neurons in the substantia nigra pars reticulata (SNr) are key basal ganglia output neurons. The activity of these neurons is critically influenced by the glutamatergic projection from the subthalamic nucleus (STN). The SNr also receives an intense serotonin (5-HT) innervation, raising the possibility that 5-HT may regulate the STN→SNr glutamatergic transmission and the consequent STN-triggered spike firing in SNr neurons. Here we show that 5-HT reduced STN stimulation-evoked long-lasting polysynaptic complex EPSCs in SNr GABA neurons. This inhibitory 5-HT effect was mimicked by the 5-HT1B receptor agonist CP93129 and blocked by the 5-HT1B antagonist NAS-181. 5-HT1A receptor ligands were ineffective. Additionally, 5-HT and CP93129 reduced the frequency but not the amplitude of miniature EPSCs, suggesting a reduced vesicular release. 5-HT and CP93129 also decreased the amplitude but increased the paired pulse ratio of the monosynaptic EPSCs in SNr GABA neurons, indicating a presynaptic 5-HT1B receptor-mediated inhibition of glutamate release. Furthermore, 5-HT and CP93129 inhibited STN-triggered burst firing in SNr GABA neurons, and CP93129's inhibitory effect was strongest when puffed to STN→SNr axon terminals in SNr, indicating a primary role of the 5-HT1B receptors in these axon terminals. Finally, the 5-HT1B receptor antagonist NAS-181 increased the STN-triggered complex EPSCs and burst firing in SNr GABA neurons, demonstrating the effects of endogenous 5-HT. These results suggest that nigral 5-HT, via presynaptic 5-HT1B receptor activation, gates the excitatory STN→SNr projection, reduces burst firing in SNr GABA neurons, and thus may play a critical role in movement control.

Introduction

The GABAergic projection neurons are the main neuronal type in the substantia nigral pars reticulata (SNr), one of the two output nuclei of the basal ganglia (Bolam et al., 2000; Deniau et al., 2007). These GABA neurons fire tonic high-frequency spikes generated by a complex interaction of intrinsic ion channels (Atherton and Bevan, 2005; Zhou et al., 2008). This tonic firing is sculpted into more meaningful motor control signals by synaptic inputs (Hikosaka et al., 2000; Zhou and Lee, 2011). One such synaptic input is the glutamatergic input from the subthalamic nucleus (STN) (Bevan et al., 1994; Parent and Hazrati, 1995; Sato et al., 2000; Parent and Parent, 2007). This glutamatergic projection provides a powerful excitatory drive that can increase the firing rate and alter the firing pattern such as inducing burst firing in SNr GABA neurons (Galati et al., 2006; Shen and Johnson, 2006; Ammari et al., 2010; Wilson and Bevan, 2011). Evidence indicates that increased firing rates and excessive bursting in SNr GABA neurons may contribute to the motor symptoms in experimental Parkinson's disease (PD) models and PD patients (Ryan and Sanders, 1993; Murer et al., 1997; Tseng et al., 2000; Steigerwald et al., 2008; Wichmann and Dostrovsky, 2011). STN lesion or functional inactivation that removes or alters the STN→SNr projection alleviates PD motor symptoms accompanied by decreased burst firing in SNr GABA neurons (Perlmutter and Mink, 2006; Maltête et al., 2007; Gubellini et al., 2009; Follett et al., 2010).

The preclinical and clinical evidence presented in the preceding section suggests that the STN-originated glutamatergic projection exerts a critical control over the intensity and pattern of SNr GABA neuron spiking activity. Consequently, mechanisms that regulate this STN→SNr projection, either at the cell body in the STN or at the axon terminal in the SNr, may influence basal ganglia output and movement control. One potential mechanism is 5-HT-mediated regulations. Anatomical studies have shown that although both the STN and the SNr receive 5-HT innervation originating in the dorsal raphe nucleus, the 5-HT innervation in the SNr is particularly dense with the 5-HT axon terminal density being twice that in the STN (Steinbusch, 1981; Moukhles et al., 1997; Parent et al., 2010, 2011; Hashemi et al., 2011). Like the intense 5-HT innervation, histochemical and ultrastructural studies have also demonstrated an intense expression of inhibitory 5-HT1B receptors in the axons but not in the somatodendritic areas in the SNr (Voigt et al., 1991; Maroteaux et al., 1992; Boschert et al., 1994; Sari et al., 1999; Riad et al., 2000; Sari, 2004). A lesion study indicated that ~50% of 5-HT1B receptors in the SNr was on striatonigral axons while the sources of the remaining 50% of the receptors were not known (Sari et al., 1999). Since

Received Aug. 27, 2012; revised Dec. 13, 2012; accepted Jan. 29, 2013.

Author contributions: S.D., L.L., and F.-M.Z. designed research; S.D., L.L., and F.-M.Z. performed research; S.D. and F.-M.Z. analyzed data; S.D. and F.-M.Z. wrote the paper.

This work was supported by NIH Grants R01NS058850 and R03NS076960 to F.M.Z. S.D. was a recipient of University of Tennessee Neuroscience Institute FY2012 fellowship. L.L. was a visiting scholar from Southern Medical University School of Basic Medical Sciences, Guangzhou, China.

The authors declare no competing financial interests.

Correspondence should be addressed to Fu-Ming Zhou, Department of Pharmacology, University of Tennessee College of Medicine, Memphis, TN 38163. E-mail: fzhou3@uthsc.edu.

DOI:10.1523/JNEUROSCI.4111-12.2013

 0270-6474/13/334875-11$15.00/0

STN neurons have a strong expression of 5-HT1B receptor mRNA, we reason that the STN→SNr axon terminals may express 5-HT1B receptors. Given the intense 5-HT innervation in the SNr, we hypothesize that these presynaptic 5-HT1B receptors may gate the STN→SNr glutamatergic projection at the axon terminal level and control the intensity of glutamatergic excitation in these basal ganglia output neurons.

Materials and Methods

Electrophysiology

Preparation of brain slices. Wild-type, 20- to 27-d-old male and female C57BL mice were used. All procedures were performed in accordance with Institutional Animal Care and Use Committee of The University of Tennessee Health Science Center and followed the guidelines of the National Institutes of Health. The procedures to prepare 10° angular sagittal slices containing the SNr, the STN, and the striatum (see Fig. 1*A*) have been described in detail (Wallmichrath and Szabo, 2002; Beurrier et al., 2006; Ammari et al., 2010). Briefly, mice were killed by decapitation under deep anesthesia, and brains were quickly dissected out and immediately immersed in oxygenated ice-cold cutting solution containing the following (in mM): 220 glycerol, 2.5 KCl, 1.25 NaH_2PO_4, 25 $NaHCO_3$, 0.5 $CaCl_2$, 7 $MgCl_2$, and 20 D-glucose. Parasagittal slices (300 μm thick) were cut using a Leica Zero Z VT1200S vibratome (Leica Microsystems) at an angle of 10°. The brain slices were transferred to a holding chamber at 34°C for 30 min in a standard artificial CSF (ACSF) containing the following (in mM): 125 NaCl, 2.5 KCl, 25 $NaHCO_3$, 1.25 NaH_2PO_4, 2.5 $CaCl_2$, 1.3 $MgCl_2$, and 10 D-glucose that was continuously bubbled with 95% O_2 and 5% CO_2. After this initial 30 min incubation at 34°C, the brain slices were kept at room temperature (25°C).

Whole-cell patch-clamp recording. Slices were placed in a recording chamber mounted on the microscope stage and continuously perfused at 2 ml/min with the standard ACSF saturated with 95% O_2 and 5% CO_2. Recordings were made at 30°C (TC 324B temperature controller; Warner Instruments) under visual guidance of a video microscope (an Olympus BX51WI and a Zeiss Axiocam MRm digital camera) equipped with Nomarski optics and a 60× water-immersion lens (Fig. 1*B*). Patch pipettes were pulled from borosilicate glass capillary tubing (KG-33, 1.1 mm inner diameter, 1.65 mm outer diameter; King Precision Glass) using a PC-10 puller (Narishige) and had resistances of 1.5–2.5 MΩ when filled with one of the following intracellular solutions. A CsCl-based intracellular solution containing the following (in mM): 135 CsCl, 0.5 EGTA, 10 HEPES, 2 Mg-ATP, 0.2 Na-GTP, and 4 Na_2-phosphocreatine, pH 7.25, 280–290 mOsm was used to record evoked complex EPSCs and miniature EPSCs (mEPSCs) in voltage-clamp recording mode. A KCl-based intracellular solution containing the following (in mM): 135 KCl, 0.5 EGTA, 10 HEPES, 2 Mg-ATP, 0.2 Na-GTP, and 4 Na_2-phosphocreatine, pH 7.25, 280–290 mOsm was used to record burst spiking activity in current-clamp recording mode. When recording evoked complex EPSCs, the Na^+ channel blocker lidocaine *N*-ethyl bromide (QX-314, 4 mM) was added to the intracellular solution to block Na spikes. mEPSCs were recorded in the presence of tetrodotoxin (TTX, 1 μM) to block action potentials. All recordings were made in the presence of 100 μM picrotoxin to block $GABA_A$ receptors.

Electrical stimulation to evoke synaptic responses. A bipolar tungsten electrode (Microprobes) was placed in the STN to activate STN→SNr glutamatergic projection and evoke complex EPSCs in SNr GABA neurons. A single pulse (0.2 ms duration) was generated by a Master-8 pulse generator (AMPI) and delivered at 0.05 Hz. The stimulation intensity was from 100 to 300 μA. To evoke monosynaptic EPSC in SNr GABA neurons, the bipolar tungsten stimulating electrode was placed within the SNr; paired pulses or a train of 10 pulses with an interpulse interval of 50 ms was generated by the Master-8 and delivered at 0.05 Hz with the stimulation intensity ranging from 10 to 50 μA.

Data acquisition and analysis. A MultiClamp 700B amplifier, pClamp 9.2 software, and Digidata 1322A interface (Molecular Devices) were used to acquire data. For voltage-clamp recording, cells were held at −70 mV. Access resistance was monitored by a 10 mV, 50 ms pulse before every evoked EPSC. Cells in which the access resistance increased by >15% were discarded. Liquid junction potential (4.8 mV for CsCl-based solution and 4.2 mV for KCl-based solution) was not corrected.

Complex EPSCs were quantified by measuring their integrated area or charge transfer using pClampfit 9.2 software. Averages of 10 consecutive complex EPSCs before or during drug administration were used to evaluate drug response. The complex EPSC area after drug administration was normalized to the predrug baseline value. Monosynaptic EPSCs were evoked by a paired pulse protocol or a 10-pulse train stimulating protocol with the stimulating electrode positioned in the SNr. The peak amplitudes of the monosynaptic EPSCs were measured using pClampfit 9.2 software. Averages of 10 consecutive monosynaptic EPSCs before or during drug administration were used to evaluate baseline and drug response, respectively. Paired pulse ratio (PPR) (for the monosynaptic EPSCs evoked by a paired pulse protocol) was calculated by dividing the peak amplitude of the second monosynaptic EPSCs by the peak amplitude of the first monosynaptic EPSCs. $EPSC_n/EPSC_1$ (for the monosynaptic EPSCs evoked by the10-pulse train stimulating protocol) was calculated by dividing the peak amplitude of the *n*th monosynaptic EPSC by the peak amplitude of the first monosynaptic EPSCs. The burst firing in SNr GABA neurons evoked by STN stimulation was quantified by measuring the average firing frequency during the 100 ms immediately after stimulation artifacts. mEPSCs were detected and analyzed by MiniAnalysis.

Drugs. All drugs were made into stock solutions in ddH_2O or dimethylsulfoxide. Stock solutions of drugs were diluted at least 1:1000 to the desired concentration in ACSF immediately before their application. Aminophosphonovalerate (APV), 6-cyano-7-nitroquinoxaline-2,3-dione (CNQX), QX-314, 5-HT, picrotoxin, CP93129, NAS-181, 8-OH-DPAT, tetrodotoxin (TTX), and WAY100135 were purchased from either Tocris Bioscience or Sigma-Aldrich. Drugs were mostly bath applied. In Figure 10, 5-HT1B agonist CP93129 was puff applied using a Picospritzer and puff pipettes with a tip diameter ~4 μm. In the SNr, the puff pipette was positioned above the tissue surface and 50–100 μm away from the neuron being recorded. In the STN, the puff pipette was positioned above the tissue surface and between the two poles of the stimulating electrode. The pressure pulse was 5 PSI and 200 ms. The pulse started 1 s before electrical synaptic stimulation to allow the drug to diffuse. Cells included in this report had stable baseline activity and drug-induced responses, thus excluding potential effects from the leaked drug.

Statistics. Data are reported as mean ± SE. The paired *t* test was used to make comparisons of evoked events before and during drug administration. Cumulative amplitude and frequency distributions of mEPSCs were compared using the Kolmogorov–Smirnov (K-S) test. One-way ANOVA with *post hoc* Bonferroni test and repeated-measures ANOVA were also used when needed. The required computation was performed using StatMost or SPSS 20. p value <0.05 was considered statistically significant.

Immunohistochemistry

The brains were fixed in 4% paraformaldehyde at 4°C overnight. Sagittal brain sections (50 μm in thickness) were cut on a Leica VT1200S vibratome. The sections then were processed for immunofluorescence detection of serotonin transporter (SERT). The free-floating sections were incubated with 2% fat-free milk, 1% bovine serum albumin (BSA), and 0.4% Triton X-100 in the PBS for 1 h at room temperature to block nonspecific binding and permeate the cell membrane, respectively. After thorough rinsing, the free-floating sections were incubated for 48 h at 4°C with the primary antibody (see below) and then rinsed in a PBS three times for 5 min each, followed by incubating with the secondary antibody (see below) for 3 h at room temperature in the dark. Both the primary and secondary antigen-antibody reactions occurred in the PBS containing 3% normal donkey serum, 1% BSA, and 0.1% Triton X-100. The primary antibody was a polyclonal SERT antibody raised in goat (Santa Cruz Biotechnology; diluted at 1:800). The secondary antibody was a donkey anti-goat IgG antibody, conjugated with red Alexa Fluor 568 (diluted at 1:200). Fluorescence images were acquired on a Zeiss 710 confocal laser scanning microscope.

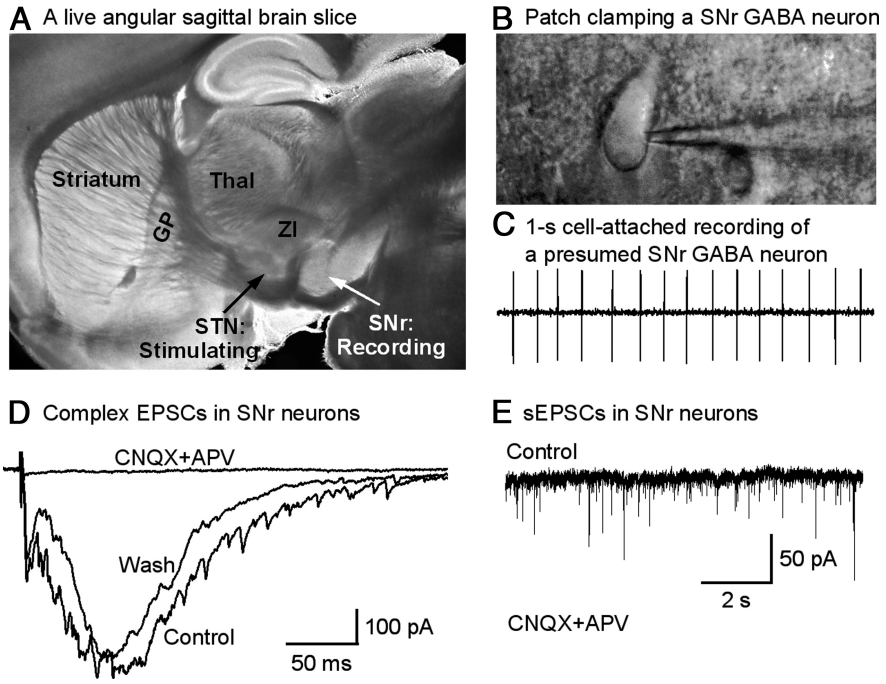

Figure 1. Focal stimulation in the STN evokes long-lasting complex EPSCs in SNr GABA neurons. ***A***, A picture of a live, 10° angular sagittal brain slice taken with a 1× objective. The SNr and STN are clearly identifiable. Other structures such as the striatum, globus pallidus (GP), thalamus (Thal), and the zona incerta (ZI) are also clearly visible and marked. ***B***, A picture, taken under a 60× objective, shows a typical SNr GABA neuron being patch-clamped in a cell-attached mode. ***C***, Typical spontaneous spikes (action potentials, ~10 Hz) in a presumed SNr GABA neuron recorded in cell-attached mode. ***D***, STN stimulation evoked long-lasting complex EPSCs in an SNr GABA neuron that were blocked by 10 μM CNQX and 20 μM APV. ***E***, sEPSCs recorded in the absence of TTX in an SNr GABA neuron were blocked by 10 μM CNQX and 20 μM APV.

Results

STN stimulation evokes complex EPSCs in SNr GABA neurons

The main neuron type in the SNr is the GABA projection neurons that fire spontaneously ~10 Hz under *in vitro* conditions (Atherton and Bevan, 2005; Ding et al., 2011a,b; Zhou and Lee, 2011). The SNr also contains sparse dopamine neurons that fire spontaneously ~1.5 Hz under similar *in vitro* conditions (Zhou et al., 2006; Ding et al., 2011a,b). Thus, we first briefly recorded action potentials in a cell-attached mode in our angular sagittal brain slices containing SNr and STN (Fig. 1*A–C*). Neurons in the SNr with a spontaneous firing rate ≥5 Hz were presumed to be GABA neurons. After cell identification, we proceeded to whole-cell recording mode and started STN stimulation to activate STN→SNr glutamatergic projection. As shown in Figure 1*D*, focal stimulation in the STN consistently evoked long-lasting, complex EPSCs in SNr GABA neurons, likely resulting from recurrent polysynaptic excitatory interactions among STN neurons, as reported by Shen and Johnson (2006, 2012) and Ammari et al. (2010). These evoked complex EPSCs and also the spontaneous EPSCs (sEPSCs) were blocked by bath-applied CNQX (10 μM) and APV (20 μM) (Fig. 1*D*,*E*), indicating that these complex EPSCs and sEPSCs were mediated by ionotropic glutamate receptors.

5-HT inhibits STN→SNr complex EPSCs

To determine the potential 5-HT regulation of the STN→SNr glutamatergic transmission, we first examined the effect of bath-applied 5-HT on the STN-triggered complex EPSCs in SNr GABA neurons. Bath-applied 5-HT should activate 5-HT receptors on both STN neuron cell bodies and axon terminals. Thus, the potential 5-HT effect on the complex EPSCs in SNr neurons should reflect the summation of potential somatic and presynaptic effects, if any. We found that bath application of 10 μM 5-HT consistently inhibited the complex EPSCs, the amplitude in particular while the duration was less affected (Fig. 2*A*,*B*). To quantify this inhibition, we calculated the area or the charge transfer of the complex EPSCs. In eight SNr GABA neurons, 10 μM 5-HT reduced the complex EPSC area to 34.2 ± 2.7% of the control, a 66% reduction ($p < 0.01$, paired *t* test). This inhibitory effect recovered upon washing out 5-HT (Fig. 2*A–C*). By applying 1, 5, 10, 20, 50, and 100 μM 5-HT, we determined that 5-HT inhibited the complex EPSCs in a dose–response manner with an IC_{50} of 4.24 μM and a Hill coefficient of 1.4, based on fitting the data points to the Hill equation (Fig. 2*D*). These results clearly indicated that 5-HT has a net inhibitory effect on the STN→SNr complex EPSCs. Next, we asked this question: Which type(s) of 5-HT receptors was mediating this inhibitory effect?

5-HT1B agonist CP93129 mimics and 5-HT1B antagonist NAS-181 inhibits the 5-HT effect on STN→SNr complex EPSCs

Among the known 5-HT receptors, only the 5-HT1 subfamily is inhibitory by coupling to $G_{i/o}$ G-protein (Bockaert et al., 2006; Hannon and Hoyer, 2008; Millan et al., 2008). Among the brain 5-HT1 receptor subtypes, only 5-HT1A and 5-HT1B receptors are expressed at substantial levels (Bruinvels et al., 1993; Barnes and Sharp, 1999). 5-HT1B receptors are known to selectively express in axon terminals while 5-HT1A receptors may be expressed at the somata and also axon terminals (Sari et al., 1999; Riad et al., 2000). Thus, we reasoned that 5-HT may inhibit complex EPSCs by activating primarily 5-HT1B receptors on STN→SNr axon terminals. To test this possibility, we first examined the effect of the 5-HT1B receptor agonist CP93129 (Li and Bayliss, 1998; Mizutani et al., 2006). As illustrated in Figure 3, *A1–A3*, bath application of 10 μM CP93129 reduced the complex EPSC area to 21.27 ± 2.52% of the control, a 79% reduction ($p < 0.001$, paired *t* test, $n = 7$ neurons), mimicking the inhibitory 5-HT effect shown in Figure 2. Furthermore, bath application of 10 μM NAS-181, a 5-HT1B receptor antagonist (Mizutani et al., 2006), blocked the effects of 10 μM 5-HT on complex EPSCs ($n = 5$ neurons; Fig. 3*B1–B3*). Together, these results indicated that 5-HT may inhibit the STN→SNr complex EPSCs through inhibitory 5-HT1B receptors.

To determine whether inhibitory 5-HT1A receptors also contribute to the 5-HT inhibition of the STN→SNr complex EPSCs, we tested the effect of 8-OH-DPAT, a 5-HT1A receptor agonist (Mizutani et al., 2006). As shown in Figure 4, *A1–A3*, 10 μM 8-OH-DPAT had no effect on STN→SNr complex EPSCs. Similarly, 10 μM WAY100135, a 5-HT1A receptor antagonist, also failed to inhibit the effect of 10 μM 5-HT on complex EPSCs (Fig. 4*B1–B3*). The fact that 5-HT1A receptor agonist 8-OH-DPAT did not mimic and 5-HT1A receptor antagonist WAY100135 did not block the effect of 5-HT on STN→SNr complex EPSCs indi-

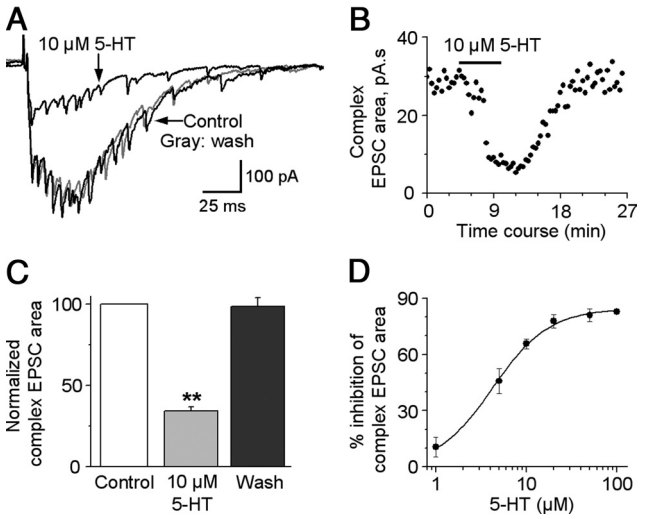

Figure 2. 5-HT inhibits STN-evoked complex EPSCs in SNr GABA neurons. ***A***, Example traces of STN-evoked complex EPSCs in an SNr GABA neuron before, during, and after bath application of 10 μM 5-HT. ***B***, Scatter plot of the complex EPSC area in the SNr GABA neuron shown in ***A*** before, during, and after bath application of 10 μM 5-HT. ***C***, Pooled data of the effects of 10 μM 5-HT on the STN-evoked complex EPSCs in eight SNr GABA neurons. ***D***, Dose–response relationship of the 5-HT inhibition of STN-evoked complex EPSCs in SNr GABA neurons. The continuous line is the fit to the Hill equation: $Y = A_*X^n[1/(K^n + X^n)]$, where A is the maximal inhibition, X is the 5-HT concentrations, K is the IC_{50}, and n is the Hill coefficient. Each data point represents 4–8 experiments. $^{**}p < 0.01$, paired t test.

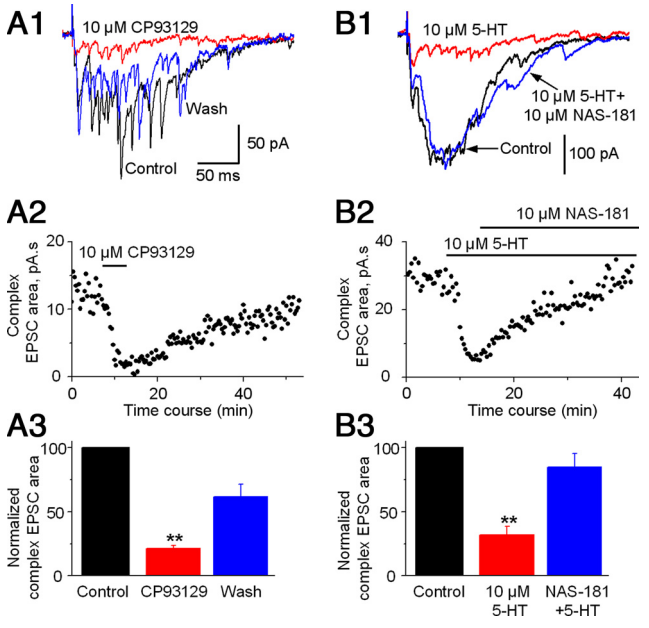

Figure 3. 5-HT1B receptors mediate the inhibitory 5-HT effect on STN-evoked complex EPSCs in SNr GABA neurons. ***A1***, Example traces of STN-evoked complex EPSCs in an SNr GABA neuron before (black trace), during (red trace), and after (blue trace) bath application of 10 μM 5-HT1B receptor agonist CP93129. ***A2***, Scatter plot of the complex EPSC area before, during, and after bath application of 10 μM CP93129 in the SNr GABA neuron shown in ***A1***. ***A3***, Pooled data for the effect of 10 μM CP93129 on the complex EPSCs (n = 7 cells). ***B1***, Example traces of the complex EPSCs in an SNr GABA neuron under control condition (black trace), during 10 μM 5-HT (red trace), and during 10 μM 5-HT + 10 μM 5-HT1B receptor antagonist NAS-181 (blue trace). The timescale in ***B1*** is the same in ***A1***. ***B2***, Scatter plot of the complex EPSC area under control condition, during 10 μM 5-HT, and during 10 μM 5-HT + 10 μM NAS-181 in the SNr GABA neuron shown in ***B1***. ***B3***, Pooled data showing 10 μM NAS-181 blocked the inhibitory 5-HT effect on the complex EPSCs (n = 5 cells). $^{**}p < 0.01$, paired t test.

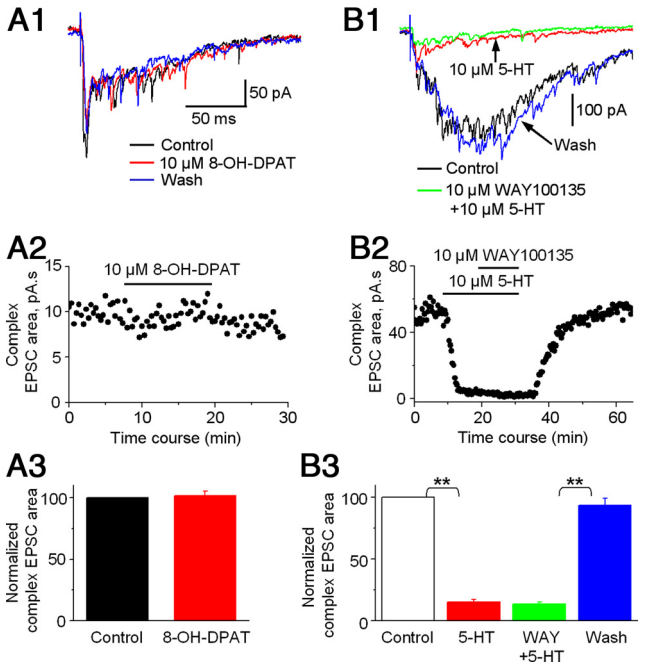

Figure 4. 5-HT1A receptor ligands do not affect STN-evoked complex EPSCs in SNr GABA neurons. ***A1***, Example traces of STN-evoked complex EPSCs in an SNr GABA neuron before (black trace), during (red trace), and after (blue trace) bath application of 10 μM 5-HT1A receptor agonist 8-OH-DPAT. ***A2***, Scatter plot of the complex EPSC area before, during, and after bath application of 10 μM 8-OH-DPAT in the SNr GABA neuron shown in ***A1***. ***A3***, Pooled data for the effect of 10 μM 8-OH-DPAT on the complex EPSCs (n = 5 cells). ***B1***, Example traces of the complex EPSCs in an SNr GABA neuron under control condition (black trace), during 10 μM 5-HT (red trace), and during 10 μM 5-HT + 10 μM 5-HT1A receptor antagonist WAY100135 (green trace), and after returning to control solution (blue trace). The timescale in ***B1*** is the same in ***A1***. ***B2***, Scatter plot of the complex EPSC area under control condition, during 10 μM 5-HT and during 10 μM 5-HT + 10 μM WAY100135, and after returning to control solution in the SNr GABA neuron shown in ***B1***. ***B3***, Pooled data showing the lack of effect of WAY100135 on the 5-HT inhibition of the complex EPSCs (n = 5). $^{**}p < 0.01$, paired t test.

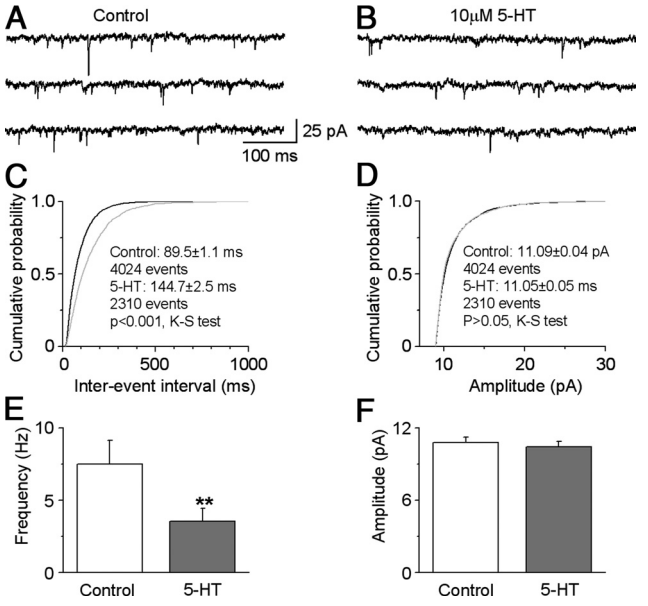

Figure 5. 5-HT reduces mEPSC frequency in SNr GABA neurons. ***A***, ***B***, Example traces showing mEPSCs recorded in an SNr GABA neuron before (***A***) and during (***B***) bath application of 10 μM 5-HT. ***C***, ***D***, Cumulative probability plots of mEPSC interevent intervals (***C***) and amplitudes (***D***), in the SNr GABA neuron shown in ***A*** and ***B***, before (black) and during 10 μM 5-HT (gray). K-S tests were used to compare the frequency and amplitude of mEPSCs in seven individual cells. ***E***, ***F***, Summary data showing 5-HT decreased the mEPSC frequency (***E***) and but not the amplitude (***F***) (n = 7 cells). $^{**}p < 0.01$, paired t test.

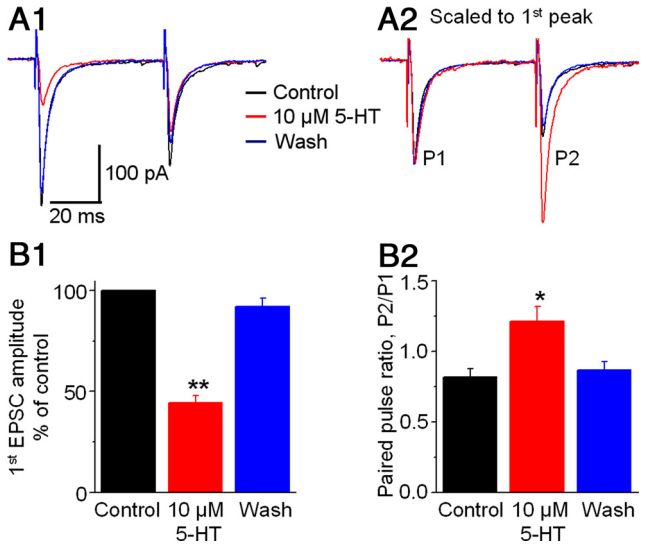

Figure 6. 5-HT inhibits locally evoked monosynaptic EPSCs in SNr GABA neurons. To avoid activating the apparent recurrent excitation among STN neurons when the stimulating electrode was placed in the STN, in this experiment, the stimulating electrode was placed in the SNr. Paired stimulating pulses were used. The interval between the two pulses was 50 ms. ***A1***, Superimposed averaged EPSCs evoked by the paired pulse stimulation before (black), during (red), and after (blue) 10 μM 5-HT application are shown in color. ***A2***, Current traces in A1 are normalized to the peak of the first EPSC in each pair to show clearly that the second EPSC is relatively increased during 10 μM 5-HT, leading to increased PPR. ***B1***, Pooled data showing the inhibitory effect of 10 μM 5-HT on the peak amplitude of the first of the paired EPSCs in seven SNr GABA neurons. ***B2***, Pooled data showing the increased PPR during 10 μM 5-HT in the seven SNr GABA neurons. *$p < 0.05$; **$p < 0.01$, paired *t* test.

cates that 5-HT1A receptors do not make detectable contribution to the 5-HT inhibition of STN→SNr complex EPSCs, further supporting the primary role for 5-HT1B receptors.

5-HT reduces the frequency of mEPSCs in SNr GABA neurons

The results in the preceding sections suggested that 5-HT inhibited the STN→SNr complex EPSCs by activating 5-HT1B receptors. Next, we asked this question: Where are these 5-HT1B receptors located? Anatomical studies have indicated that 5-HT1B receptors are commonly located on the presynaptic terminals (Boschert et al., 1994; Sari et al., 1999; Riad et al., 2000; Sari, 2004). So we reasoned that 5-HT may activate presynaptic 5-HT1B receptors to inhibit the STN→SNr complex EPSCs. To answer this question, we studied the effect of 5-HT on mEPSCs in SNr GABA neurons, since the frequency of mEPSCs is an indication of vesicular neurotransmitter release, whereas the amplitude of mEPSCs is largely a reflection of postsynaptic glutamate receptors (Sudhof, 2004). mEPSCs were recorded in the presence of 1 μM TTX. Indeed, as illustrated in Figure 5, *A–F*, bath application of 10 μM 5-HT decreased the frequency of mEPSCs in SNr GABA neurons from 7.51 ± 1.64 to 3.53 ± 0.89 Hz, a 53% decrease ($p < 0.01$, paired *t* test, $n = 7$ neurons). In contrast, the amplitude of these mEPSCs was not affected (10.80 ± 0.46 pA and 10.43 ± 0.44 pA for before and during bath application of 5-HT, respectively, $p > 0.05$, paired *t* test, $n = 7$ neurons). The 5-HT1B receptor agonist CP93129 had similar effects ($n = 3$ cells). These results indicated that 5-HT inhibited complex EPSCs by activating the inhibitory 5-HT1B receptors on the STN→SNr axon terminals in the SNr, leading to reduced vesicular neurotransmitter release.

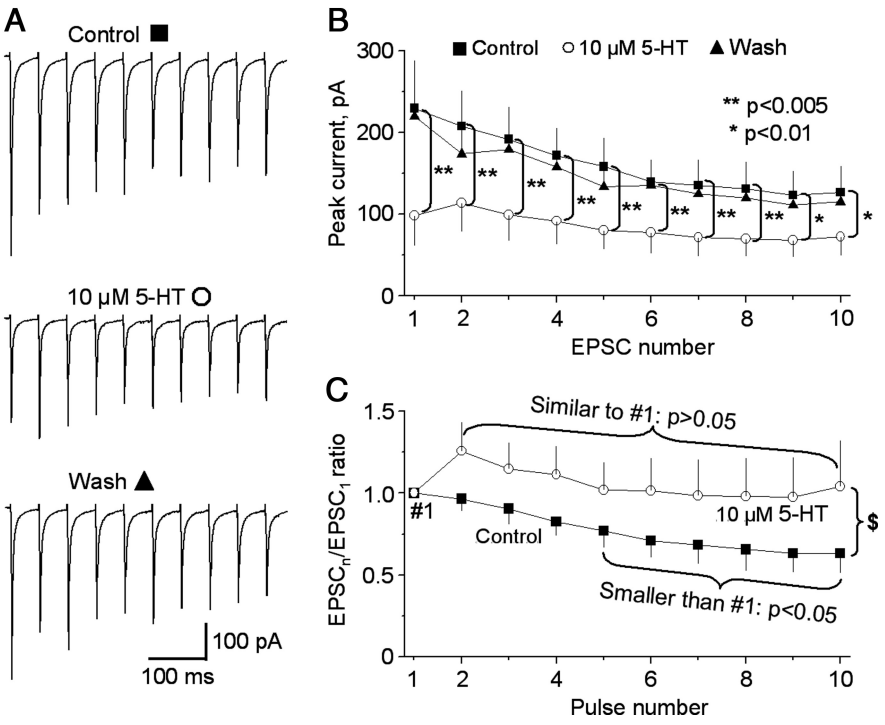

Figure 7. 5-HT reduces the intensity and variation of monosynaptic STN→SNr EPSCs in SNr GABA neurons. The stimulating electrode was placed in the SNr. A train of 10 stimulating pulses with interpulse interval of 50 ms were used. ***A***, Averaged EPSCs evoked by the train of 10 pulse stimulation before and during 10 μM 5-HT application. ***B***, Pooled data showing the inhibitory effect of 10 μM 5-HT on the peak amplitude of a train of 10 EPSCs in eight SNr GABA neurons. ***C***, Pooled data showing the increased ratios of $EPSC_n/EPSC_1$ in the eight SNr GABA neurons during 10 μM 5-HT application. Recovery data were not shown for clarity of the graph. $, $p < 0.05$ for the ratios of $EPSC_2/EPSC_1$ through $EPSC_{10}/EPSC_1$ under control versus during 10 μM 5-HT. Repeated-measures ANOVA was used.

5-HT inhibits monosynaptic STN→SNr EPSCs in SNr GABA neurons

We further tested the idea of inhibitory presynaptic 5-HT receptors on STN→SNr axon terminals by studying the effect of 5-HT on monosynaptic EPSCs in SNr GABA neurons evoked by a paired pulse protocol with the stimulating electrode placed in the SNr to avoid activating intra-STN recurrent excitation. As shown in Figure 6, *A1* and *B1*, bath application of 10 μM 5-HT reduced the peak amplitude of the first of the paired EPSCs to 44.4 ± 3.5% of the control, a 56% decrease ($p < 0.01$, paired *t* test, $n = 7$). Meanwhile, 10 μM 5-HT reduced the peak amplitude of the second of the paired EPSCs to a less extent, thus increasing the PPR from 0.83 ± 0.07 under control to 1.21 ± 0.11 during 5-HT application ($p < 0.05$, paired *t* test, $n = 7$) (Fig. 6*A2*,*B2*). The 5-HT1B agonist CP93129 had similar effects ($n = 4$ cells). Since an increased PPR is an indication of inhibition of presynaptic vesicular release (Dittman et al., 2000; Thomson, 2000; Zucker and Regehr, 2002; Fioravante and Regehr, 2011), these results further suggest a presynaptic 5-HT1B receptor-mediated mechanism underlying the inhibitory 5-HT effect on STN→SNr EPSCs. Also, unlike the long-lasting complex EPSC that trig-

gered ~10 spikes within the 100 ms period after stimulation (described in the next section), a monosynaptic EPSC was able to trigger only 1–3 spikes in SNr GABA neurons, indicating the importance of the STN projection and its 5-HT inhibition in the regulation of SNr GABA neuron activity.

Next, we asked this question: How does 5-HT affect a train of synaptic input? To answer this question, we stimulated SNr with a train of 10 pulses with interpulse interval of 50 ms (20 Hz) and examined the effect of 10 μM 5-HT on the evoked monosynaptic EPSCs. We made statistical comparisons on these repetitive stimulation-evoked EPSCs using repeated-measures ANOVA. As illustrated in Figure 7, *A–C*, under control condition, 20 Hz repetitive stimulation-evoked monosynaptic EPSCs displayed significant activity-dependent depression. Consequently, the ratios of fifth EPSC/first EPSC through tenth EPSC/first EPSC were smaller than the ratio (1.0) of first EPSC/first EPSC (Fig. 7*C*). Bath application of 10 μM 5-HT induced a global decrease in the peak currents of the EPSC train ($n = 8$ cells, $p < 0.01$, repeated-measures ANOVA; Fig. 7*A*,*B*). The first EPSC in the train was most severely reduced, decreasing from 229.5 ± 58.1 to 98.2 ± 35.5 pA ($p = 0.002$, repeated-measures ANOVA, $n = 8$ cells), a 59% reduction. This led to less variable peaks in the EPSC train. Consequently, the ratios of $EPSC_n/EPSC_1$ increased significantly during bath application of 10 μM 5-HT ($p = 0.022$, repeated-measures ANOVA, $n = 8$ cells) (Fig. 7*C*). For example, under our control condition, the ratio of $EPSC_{10}/EPSC_1$ was 0.63 ± 0.12 and smaller than the ratio (1.0) of $EPSC_1/EPSC_1$ ($p = 0.015$, repeated-measures ANOVA), indicating that the monosynaptic EPSCs underwent activity-dependent depression, likely due to a decrease in the synaptic vesicle release during repetitive stimulation (Thomson, 2000; Zucker and Regehr, 2002). During bath application of 10 μM 5-HT, there was no difference between the ratios of $EPSC_1/EPSC_1$ (1.0) and $EPSC_{10}/EPSC_1$ (1.04 ± 0.28) ($p = 0.891$, repeated-measures ANOVA), indicating an equalization of EPSC amplitudes. These results suggested that 5-HT can reduce the intensity of the subthalamonigral excitation by reducing the glutamate release, leading to a more moderate and more even excitatory synaptic transmission during repetitive STN neuron firing.

5-HT and 5HT1B receptor agonist CP93129 inhibit STN-triggered burst firing in SNr GABA neurons

The STN can trigger burst firing in SNr GABA neurons (Shen and Johnson, 2006; Ammari et al., 2010). Our voltage-clamp data indicated that 5-HT inhibits the STN→SNr complex EPSCs through the presynaptic 5-HT1B receptors. So we predicted that 5-HT may inhibit STN-triggered burst firing in SNr GABA neurons. As shown in Figure 8, *A* and *B*, bath application of 10 μM 5-HT decreased the STN-triggered burst firing frequency in the 100 ms period after the stimulation artifact from 92.63 ± 11.40 to 38.11 ± 5.42 Hz ($p < 0.01$, paired *t* test, $n = 6$). This effect was recovered upon washing out 5-HT. At the same time, 10 μM 5-HT also significantly increased the spontaneous firing frequency in SNr GABA neurons from the baseline 8.51 ± 0.59 to 13.93 ± 1.86 Hz ($p < 0.05$, paired *t* test, $n = 6$) (Fig. 8*C*), likely due to 5-HT activating 5-HT2C receptors in SNr GABA neurons (Stanford and Lacey, 1996). These results indicated that 5-HT inhibited STN-triggered burst firing in SNr GABA neurons while increasing the spontaneous firing frequency that tends to increase the firing regularity in these neurons (Zhou et al., 2008).

We also tested the effect of the 5-HT1B receptor agonist CP93129 on STN-triggered burst firing in SNr GABA neurons. As illustrated in Figure 9, *A* and *B*, bath application of 10 μM CP93129 decreased the average burst firing frequency in the 100 ms period immediately after the stimulation artifact from 88.73 ± 15.91 to 33.26 ± 7.14 Hz ($p < 0.005$, paired *t* test, $n = 6$). However, in these same cells, 10 μM CP93129 had no effect on the baseline spontaneous firing frequency (11.97 ± 2.26 and 10.59 ± 2.37 Hz for control and 10 μM CP93129 respectively, $p = 0.28$, paired *t* test, $n = 6$) (Fig. 9*C*). These results indicated that 5-HT1B receptor activation may inhibit STN-triggered burst fir-

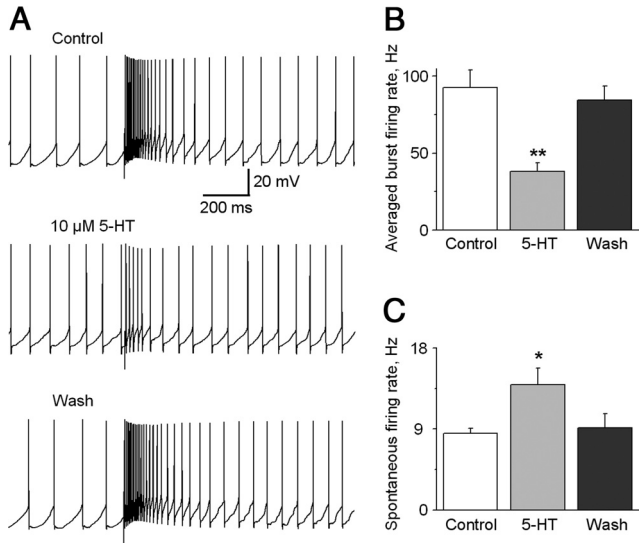

Figure 8. 5-HT inhibits STN-triggered burst firing in SNr GABA neurons. ***A***, Example traces show the STN-triggered burst firing in SNr GABA neurons under control condition, during bath application of 10 μM 5-HT, and after washing out 5-HT. ***B***, Summary of the inhibitory effect of 10 μM 5-HT on the average intraburst firing frequency during the 100 ms immediately following the stimulus artifact in six SNr GABA neurons. ***C***, Summary of the excitatory effect of 10 μM 5-HT on the spontaneous firing frequency in the six same SNr GABA neurons. *$p < 0.05$; **$p < 0.01$, paired *t* test.

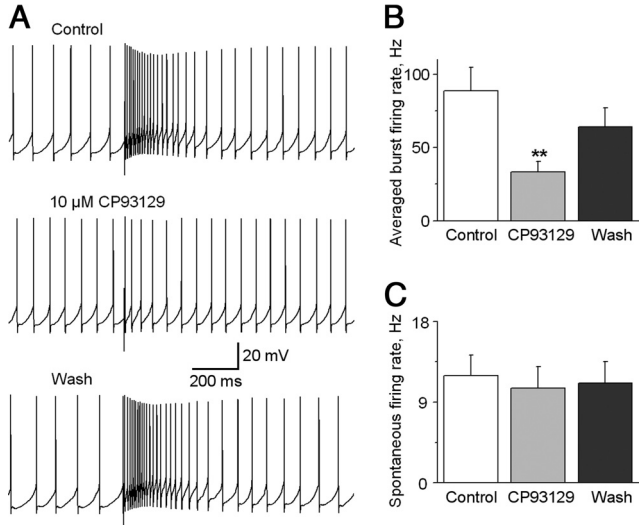

Figure 9. 5-HT1B receptor agonism inhibits STN-triggered burst firing in SNr GABA neurons. ***A***, Example traces show STN-triggered burst firing in an SNr GABA neuron under control condition, during bath application of 10 μM CP93129, and after washing out CP93129. ***B***, Summary of the inhibitory effect of 10 μM CP93129 on the average intraburst firing frequency during the 100 ms immediately following the stimulus artifact in six SNr GABA neurons; 10 μM CP93129 significantly inhibited the averaged burst firing frequency. ***C***, Summary of the excitatory effect of 10 μM CP93129 on the spontaneous firing frequency in the six same SNr GABA neurons. **$p < 0.01$, paired *t* test.

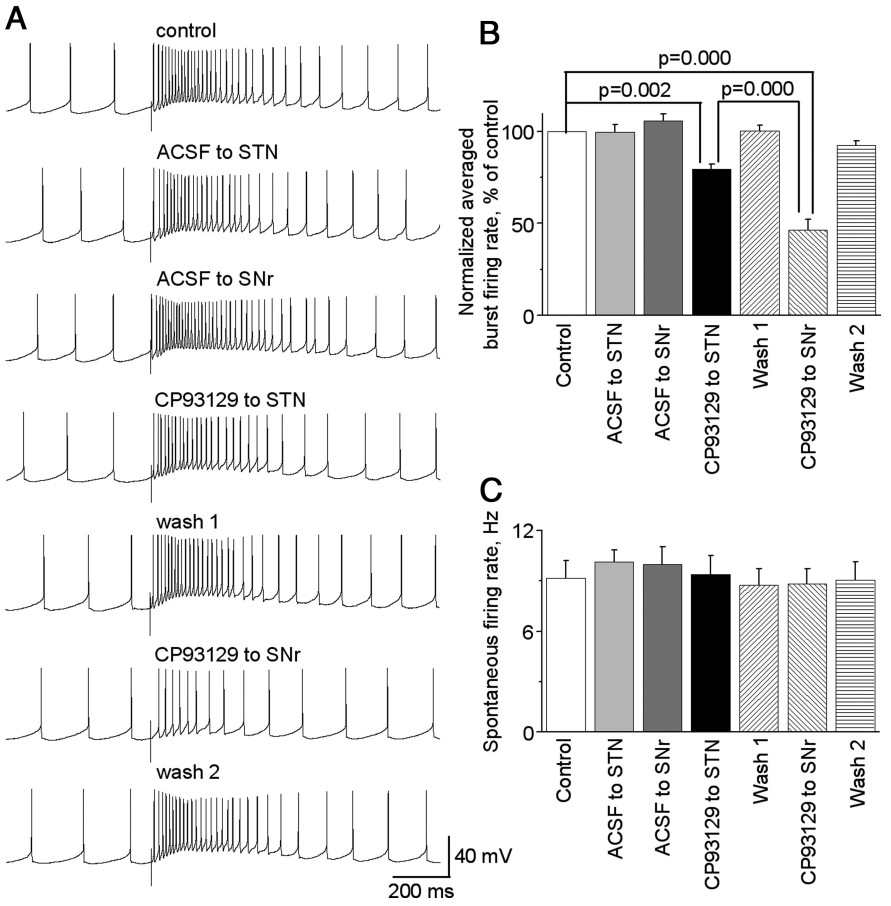

Figure 10. 5-HT1B receptor agonist CP93129 inhibits STN-triggered burst firing in SNr GABA neurons more strongly when applied locally to SNr than to STN. ***A***, Example traces show STN-triggered burst firing in an SNr GABA neuron under control condition, locally puffed ACSF, or 1 mM CP93129 to STN or SNr, locally and washing out CP93129. ***B***, Pooled data showing the effect of locally puffed ACSF or 1 mM CP93129 to SNr or STN on STN-triggered burst firing rate in SNr GABA neurons. The averaged burst firing rates in different treatment conditions were normalized to the averaged burst firing rate in control. Locally puffed 1 mM CP93129 to SNr reduced the averaged bursting firing rate to a larger extent than did locally puffed 1 mM CP93129 to STN ($n = 8$, $p = 0.000$), while locally puffed ACSF to STN or SNr had no effect on the burst firing rate ($n = 5$, $p = 1.000$). ***C***, Summary of the lack of effect of locally puffed ACSF ($n = 5$, $p = 1.000$) or 1 mM CP93129 ($n = 8$, $p = 1.000$) to STN or SNr on the spontaneous firing frequency in the same SNr GABA neurons. *Post hoc* Bonferroni test following one-way ANOVA was used for statistical comparison.

ing in SNr GABA neurons while sparing the intrinsically generated baseline spontaneous firing in these neurons.

To further test the idea that activation of 5-HT1B receptor on the STN→SNr axon terminal is mainly responsible for reducing the STN-triggered burst firing in SNr GABA neurons, we locally puffed 1 mM CP93129 to STN and SNr, respectively, using a picospritzer. In STN, the puff pipette was positioned between the two poles of the stimulating electrode such that the ejected drug can quickly reach the tissue being stimulated electrically. In SNr, the puff pipette was positioned ~75 μm away from the recorded neuron. More details are described in the method section. As shown in Figure 10, *A* and *B*, locally puffed 1 mM CP93129 to STN significantly but modestly reduced the average burst firing rate to 79.5 ± 2.9% of control, a 20% reduction ($n = 8$, $p = 0.002$, *post hoc* Bonferroni test following one-way ANOVA, $F_{(6,43)} = 34.9$, $p < 0.001$). Locally puffed 1 mM CP93129 to SNr significantly decreased the average burst firing rate to 46.3 ± 5.8% of control, a 54% reduction ($n = 8$, $p = 0.000$, one-way ANOVA). The inhibitory effect on the average burst firing rate induced by 1 mM CP93129 puffed to SNr is statistically larger than the inhibition induced by 1 mM CP93129 puffed to STN ($n = 8$, $p = 0.00$, *post hoc* Bonferroni test following one-way ANOVA; Fig. 10*B*). Similar to the results of bath application of CP93129, locally puffed 1 mM CP93129 to both STN and SNr had no effect on the baseline spontaneous firing (9.2 ± 1.0, 9.4 ± 1.1, and 8.8 ± 0.9 Hz for control; locally puffed 1 mM CP93129 to STN and locally puffed 1 mM CP93129 to SNr, respectively; $n = 8$, one-way ANOVA: $F_{(6,43)} = 0.63$, $p = 0.71$). Furthermore, increasing CP93129 to 2 mM in the puff pipette did not increase its inhibitory effect in STN or SNr, whereas decreasing CP93129 to 0.2 mM led to a smaller effect. Thus, puff applied 1 mM CP93129 apparently saturated the 5-HT1B receptors in STN and SNr (data not shown). To rule out any potential nonspecific effect of puff application, we also puffed the normal extracellular solution or the ACSF (used to dissolve CP93129) to STN and SNr during the recording of five of the eight SNr neurons described above. As shown in Figure 10, *A–C*, locally puffed ACSF to STN or SNr had no effect on both averaged burst firing and spontaneous firing rate ($n = 5$, one-way ANOVA, $p = 1.000$ for both averaged burst firing and spontaneous firing). Together, these results indicate that activation of 5-HT1B receptor on the STN→SNr axon terminal is mainly responsible for reducing the STN-triggered burst firing in SNr GABA neurons.

Endogenous 5-HT effect on STN→SNr complex EPSCs and STN-triggered burst firing in SNr GABA neurons

Since the SNr receives a dense 5-HT innervation (Fig. 11*A*), we reasoned that 5-HT axons in our sagittal brain slices may release sufficient amounts of 5-HT that in turn activate presynaptic 5-HT1B receptors and inhibit glutamate release from the STN→SNr projection. To test this idea, we examined the effect of the 5-HT1B receptor antagonist NAS-181. As illustrated in Figure 11, *B* and *C*, bath application of 10 μM NAS-181 increased the STN→SNr complex EPSC area by 20.3 ± 3.2% ($p < 0.05$, paired *t* test, $n = 5$ cells), and the effect was recovered upon washing out NAS-181. Equally important, under current-clamp recording mode, bath application of 10 μM NAS-181 increased STN stimulation-triggered burst firing frequency in the 100 ms period immediately after the stimulation to 95.4 ± 10.0 Hz from 75.6 ± 7.8 Hz under control ($p < 0.05$, paired *t* test, $n = 6$; Fig. 12*A*,*B*). The spontaneous spike firing was not affected, remaining ~10 Hz (Fig. 12*A*,*C*), consistent with the idea that the spontaneous baseline spike firing was intrinsically generated and not driven by synaptic inputs (Atherton and Bevan, 2005; Zhou and Lee, 2011) and that 5-HT1B receptors are on STN→SNr axon terminals as indicated by our data presented in the preceding sections. These results indicate that the STN→SNr glutamatergic transmission is inhibited by endogenous 5-HT in the SNr.

Discussion

The main findings of this study are that 5-HT may inhibit or gate the STN→SNr glutamatergic projection by reducing glutamate release via presynaptic 5-HT1B receptors, consequently decreasing STN-triggered burst firing and global firing intensity in SNr projection neurons. These findings advance our understanding of this crucial excitatory drive known to be important to the function of the basal ganglia and movement disorders such as PD.

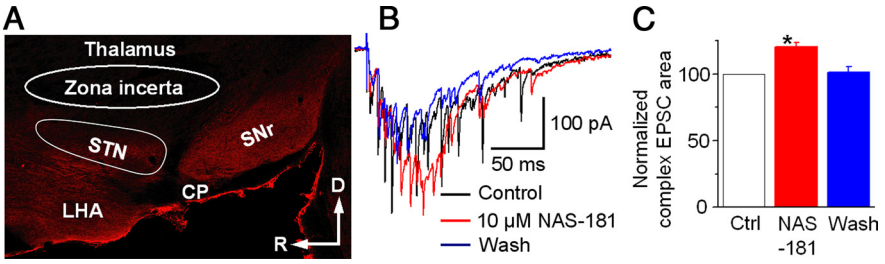

Figure 11. 5-HT1B receptor antagonism enhances STN-evoked complex EPSCs in SNr GABA neurons. ***A***, A sagittal brain section showing the intense 5-HT innervation in the SNr revealed by immunostaining for the 5-HT transporter protein. CP, cerebral peduncle; LHA, lateral hypothalamus; D, dorsal; R, rostral. ***B***, Example traces of STN-evoked complex EPSCs in an SNr GABA neuron before (black), during (red), and after (blue) bath application of 10 μM NAS-181. ***C***, Pooled data showing that bath application of 10 μM NAS-181 increased the complex EPSC area in five SNr GABA neurons. *$p < 0.05$, paired *t* test.

Presynaptic 5-HT1B receptor-mediated gating of the STN→SNr glutamatergic projection

Anatomical studies have provided strong evidence that STN neurons project directly or monosynaptically to the SNr (Kita and Kitai, 1987; Smith et al., 1990; Bevan et al., 1994; Sato et al., 2000; Parent and Parent, 2007). There is also evidence that STN may project to the pedunculopontine nucleus (PPN), which in turn projects back to STN, though the neurochemical nature of this projection is not clear (Hammond et al., 1983; Jackson and Crossman, 1983; Kita and Kitai, 1987; Smith et al., 1990; Martinez-Gonzalez et al., 2011). The relatively long distance STN projection to PPN was likely to be severely cut in our slice preparation. Furthermore, in a subset of our experiments, cutting off PPN caused no difference in STN-evoked EPSCs in SNr GABA neurons. Studies have also established that STN neurons and thus STN efferents use glutamate as their neurotransmitter (Smith and Parent, 1988; Parent and Hazrati, 1995; Shen and Johnson, 2006; Ammari et al., 2010). Therefore, when we stimulated STN in our brain slice preparation, we activated predominately the STN→SNr monosynaptic glutamatergic projection and intra-STN polysynaptic recurrent glutamatergic excitation.

The importance of STN in basal ganglia physiology and pathophysiology is demonstrated by that fact that STN is the most common target of deep brain stimulation, which has a dramatic therapeutic effect on the motor symptoms of PD and related motor disorders (Perlmutter and Mink, 2006; Gubellini et al., 2009; Lozano et al., 2010). Therefore, understanding the endogenous mechanisms that regulate the STN output is essential. In our present study, we found that 10 μM 5-HT reduced the area or charge transfer of the complex STN→SNr EPSC by 66% (Fig. 2). The 5-HT1B receptor agonist CP93129 mimicked and 5-HT1B antagonist NAS-181 blocked this 5-HT effect, whereas ligands for 5-HT1A receptors were without effect (Figs. 3, 4). Further, 10 μM 5-HT reduced mEPSC frequency by 53% and the monosynaptic STN→SNr EPSC amplitude by 56% while increasing PPR by 46% (Figs. 5, 6). Thus, the majority (80–85%) of 5-HT inhibition of the STN→SNr complex EPSCs was mediated by presynaptic 5-HT1B receptors in STN→SNr axon terminals, while the 15–20% of the 5-HT inhibition was likely due to 5-HT1B-mediated inhibition of intra-STN recurrent excitation. This conclusion was further supported by our observation that 5-HT1B agonist CP93129 puffed to SNr reduced the averaged burst firing rate to a larger extent than CP93129 puffed to STN (a 54% reduction vs a 20% reduction) (Fig. 7). Our present observations and interpretation are fully consistent with anatomical studies on 5-HT1B receptor expression. These studies, using mRNA *in situ* hybridization, receptor ligand binding, receptor immunostain, and ultrastructural techniques, have established that the expression of 5-HT1B receptors is the strongest in the SNr and a few other brain areas (Bruinvels et al., 1993, 1994; Boschert et al., 1994; Sari et al., 1999; Riad et al., 2000; Sari, 2004). These studies also indicate that 5-HT1B receptors are located in axon terminals and preterminal areas, but not in somatodendritic areas. Lesion of the striatum reduced the 5-HT1B receptor level in the SNr by ~50%, indicating that 5-HT1B receptors are on the striatonigral axons (Stanford and Lacey, 1996; Sari et al., 1999) and also other afferents to the SNr (Sari et al., 1999). One afferent that may express 5-HT1B receptors is the STN→SNr glutamatergic projection. Like striatonigral neurons, STN neurons express a high level of 5-HT1B mRNA but not 5-HT1B receptors, a typical mismatch of 5-HT1B mRNA level and 5-HT1B receptor level at the cell body (Maroteaux et al., 1992; Boschert et al., 1994; Sari, 2004). Although direct ultrastructural evidence showing 5-HT1B receptors being at STN→SNr axon terminals is not yet available, we speculate that like striatonigral neurons, STN neurons may express high levels of 5-HT1B receptors at their axon terminals to reduce the release of glutamate. This conclusion, coupled with the fact that the SNr has an intense

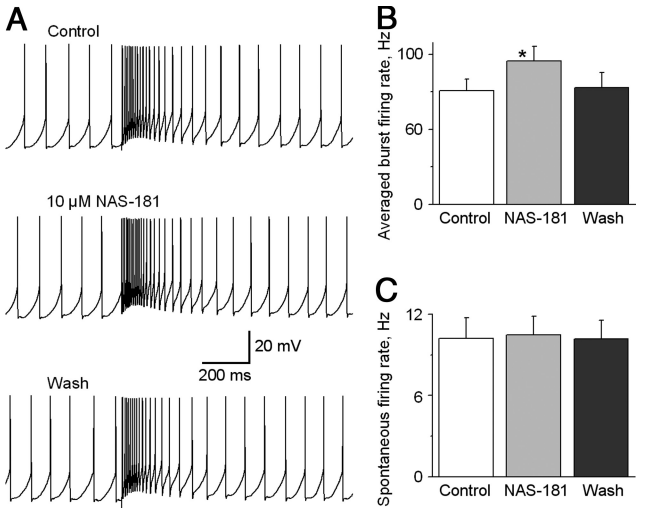

Figure 12. 5-HT1B receptor antagonism increases STN-triggered burst firing in SNr GABA neurons. ***A***, Example traces show STN-triggered burst firing in an SNr GABA neuron under control condition, during bath application of 10 μM 5-HT1B receptor antagonist NAS-181, and after washing out NAS-181. ***B***, Summary of the excitatory effect of 10 μM NAS-181 on the average intraburst firing frequency during the 100 ms immediately following the stimulus artifact in six SNr GABA neurons. ***C***, Summary of the lack of effect of 10 μM NAS-181 on the spontaneous firing frequency in the six same SNr GABA neurons. *$p < 0.05$, paired *t* test.

5-HT innervation (Moukhles et al., 1997; Parent et al., 2011), leads us to speculate that in intact animals, the endogenous 5-HT in the STN-SNr region affects STN→SNr glutamatergic synaptic transmission predominantly by directly inhibiting glutamate release at the axon terminal. The contribution from 5-HT regulation of STN neuron somata may be relatively small.

Our present results that 5-HT1B receptor activation reduces glutamate release at STN→SNr axon terminals are consistent with literature reports that 5-HT1B receptors are coupled to $G_{i/o}$ G-protein, leading a reduction of the intracellular cAMP level (Bockaert et al., 2006; Hannon and Hoyer, 2008; Millan et al., 2008). A decreased cAMP level may reduce neurotransmitter release (Yao and Sakaba, 2010) by either decreasing Ca^{2+} influx or decreasing the efficacy of presynaptic secretory machinery (Chen and Regehr, 1997; Kaneko and Takahashi, 2004). Our results are also consistent with reported presynaptic 5-HT1B receptor inhibition of glutamate release at other synapses (Singer et al., 1996; Li and Bayliss, 1998; Muramatsu et al., 1998; Pickard et al., 1999; Morikawa et al., 2000; Laurent et al., 2002; Bouryi and Lewis, 2003; Mizutani et al., 2006). The lack of effect of 5-HT1A receptor ligands in our present study is consistent with anatomical findings that indicated a lack of detectable 5-HT1A receptor expression in the SNr (Kia et al., 1996; Riad et al., 2000). Also, despite the reported expression of 5-HT4 and 5-HT2C receptors in the STN (Pompeiano et al., 1994; Xiang et al., 2005; Shen and Johnson, 2007), we did not detect any significant effect of 5-HT2C and 5-HT4 receptor agonists on STN→SNr complex EPSCs (data not shown). These results suggest that 5-HT2C and 5-HT4 receptors may be expressed at relatively low levels in the STN neurons (Clemett et al., 2000) that do not produce detectable effects on the interaction among STN neurons and thus no effect on the generation of the complex EPSCs, under our experimental conditions. Together, our results indicate that presynaptic 5-HT1B receptors gate the STN→SNr glutamatergic projection.

5-HT inhibits STN-triggered burst firing in SNr GABA neurons: functional implications

In this study, we found that focal stimulation in the STN evokes long-lasting complex EPSCs that trigger bursts of high-frequency spiking or burst firing in SNr GABA neurons (Figs. 8, 9), showing a powerful excitatory influence of the glutamatergic STN projection on SNr GABA neurons. This finding is consistent with previous studies that described similar STN neuron recurrent excitation-triggered complex EPSCs and burst firing in SNr GABA neurons (Shen and Johnson, 2006; Ammari et al., 2010). Equally important, we also found that 5-HT and 5-HT1B receptor agonist CP93129 inhibited STN-triggered burst firing (Figs. 8–10). This inhibitory effect was likely the result of presynaptic 5-HT1B receptors inhibiting glutamate release, as discussed in the preceding section. Thus, endogenous 5-HT, via presynaptic 5-HT1B receptors on STN-SNr axon terminals, may dampen excitatory inputs from the STN and reduce the burstiness in the spike firing in SNr GABA neurons that is known to have potential pathophysiological relevance (Zhou and Lee, 2011).

Given the known importance of the STN in motor control and PD pathophysiology (Obeso et al., 2008; Baunez et al., 2011), the presynaptic 5-HT inhibition of the STN glutamatergic projection described here may have critical functional implications. First, our finding provides a cellular substrate to the view that a key function of the brain 5-HT system is to facilitate motor activity (Jacobs and Fornal, 1999; Jacobs et al., 2002), because 5-HT inhibition of the STN→SNr glutamatergic projection may lead to a relative disinhibition of the thalamocortical motor circuit and thus promote movements. The second implication is the potential contribution of this presynaptic 5-HT1B receptor-mediated mechanism to the pathophysiology of PD. A well established neurophysiological abnormality in PD models and PD patients is that the STN neurons fire at increased frequencies and with increased bursting, causing heightened and abnormal STN→SNr glutamatergic transmission (Steigerwald et al., 2008; Lozano et al., 2010; Wichmann and Dostrovsky, 2011; Wichmann et al., 2011). This causes the basal ganglia GABA output neurons in the SNr to increase their spike frequency and burst firing that in turn result in an abnormal inhibition of the thalamocortical motor circuit and parkinsonian motor deficits. Postmortem studies have shown a substantial degeneration of the 5-HT system in PD brains, indicating a potentially important role of the 5-HT system in the pathophysiology of PD (Braak et al., 2004; Kish et al., 2008; Huot et al., 2011). A loss of 5-HT in the SNr in the PD brain may weaken the inhibitory 5-HT control over the STN→SNr projection, potentially leading to increased firing with abnormal patterns in SNr GABA neurons and eventually motor deficits. Indeed, a recent study has demonstrated that 5-HT depletion increased burst firing in SNr GABA neurons (Delaville et al., 2012). Our results also indicate that the presynaptic 5-HT1B receptors on the STN→SNr axon terminals may be an important target for treating PD motor deficits.

References

Ammari R, Lopez C, Bioulac B, Garcia L, Hammond C (2010) Subthalamic nucleus evokes similar long lasting glutamatergic excitations in pallidal, entopeduncular and nigral neurons in the basal ganglia slice. Neuroscience 166:808–818. CrossRef Medline

Atherton JF, Bevan MD (2005) Ionic mechanisms underlying autonomous action potential generation in the somata and dendrites of GABAergic substantia nigra pars reticulata neurons *in vitro*. J Neurosci 25:8272–8281. CrossRef Medline

Barnes NM, Sharp T (1999) A review of central 5-HT receptors and their function. Neuropharmacology 38:1083–1152. CrossRef Medline

Baunez C, Yelnik J, Mallet L (2011) Six questions on the subthalamic nucleus: lessons from animal models and from stimulated patients. Neuroscience 198:193–204. CrossRef Medline

Beurrier C, Ben-Ari Y, Hammond C (2006) Preservation of the direct and indirect pathways in an in vitro preparation of the mouse basal ganglia. Neuroscience 140:77–86. CrossRef Medline

Bevan MD, Bolam JP, Crossman AR (1994) Convergent synaptic input from the neostriatum and the subthalamus onto identified nigrothalamic neurons in the rat. Eur J Neurosci 6:320–334. CrossRef Medline

Bockaert J, Claeysen S, Bécamel C, Dumuis A, Marin P (2006) Neuronal 5-HT metabotropic receptors: fine-tuning of their structure, signaling, and roles in synaptic modulation. Cell Tissue Res 326:553–572. CrossRef Medline

Bolam JP, Hanley JJ, Booth PA, Bevan MD (2000) Synaptic organisation of the basal ganglia. J Anat 196:527–542. CrossRef Medline

Boschert U, Amara DA, Segu L, Hen R (1994) The mouse 5-hydroxytryptamine1B receptor is localized predominantly on axon terminals. Neuroscience 58:167–182. CrossRef Medline

Bouryi VA, Lewis DI (2003) The modulation by 5-HT of glutamatergic inputs from the raphe pallidus to rat hypoglossal motoneurones, in vitro. J Physiol 553:1019–1031. CrossRef Medline

Braak H, Ghebremedhin E, Rüb U, Bratzke H, Del Tredici K (2004) Stages in the development of Parkinson's disease-related pathology. Cell Tissue Res 318:121–134. CrossRef Medline

Bruinvels AT, Palacios JM, Hoyer D (1993) Autoradiographic characterisation and localisation of 5-HT1D compared to 5-HT1B binding sites in rat brain. Naunyn Schmiedebergs Arch Pharmacol 347:569–582. CrossRef Medline

Bruinvels AT, Landwehrmeyer B, Gustafson EL, Durkin MM, Mengod G, Branchek TA, Hoyer D, Palacios JM (1994) Localization of 5-HT1B, 5-HT1D alpha, 5-HT1E and 5-HT1F receptor messenger RNA in rodent and primate brain. Neuropharmacology 33:367–386. CrossRef Medline

Chen C, Regehr WG (1997) The mechanism of cAMP-mediated enhancement at a cerebellar synapse. J Neurosci 17:8687–8694. Medline

Clemett DA, Punhani T, Duxon MS, Blackburn TP, Fone KC (2000) Immunohistochemical localisation of the 5-HT2C receptor protein in the rat CNS. Neuropharmacology 39:123–132. CrossRef Medline

Delaville C, Navailles S, Benazzouz A (2012) Effects of noradrenaline and serotonin depletions on the neuronal activity of globus pallidus and substantia nigra pars reticulata in experimental parkinsonism. Neuroscience 202:424–433. CrossRef Medline

Deniau JM, Mailly P, Maurice N, Charpier S (2007) The pars reticulata of the substantia nigra: a window to basal ganglia output. Prog Brain Res 160:151–172. CrossRef Medline

Ding S, Matta SG, Zhou FM (2011a) Kv3-like potassium channels are required for sustained high-frequency firing in basal ganglia output neurons. J Neurophysiol 105:554–570. CrossRef Medline

Ding S, Wei W, Zhou FM (2011b) Molecular and functional differences in voltage-activated sodium currents between GABA projection neurons and dopamine neurons in the substantia nigra. J Neurophysiol 106:3019–3034. CrossRef Medline

Dittman JS, Kreitzer AC, Regehr WG (2000) Interplay between facilitation, depression, and residual calcium at three presynaptic terminals. J Neurosci 20:1374–1385. Medline

Fioravante D, Regehr WG (2011) Short-term forms of presynaptic plasticity. Curr Opin Neurobiol 21:269–274. CrossRef Medline

Follett KA, Weaver FM, Stern M, Hur K, Harris CL, Luo P, Marks WJ Jr, Rothlind J, Sagher O, Moy C, Pahwa R, Burchiel K, Hogarth P, Lai EC, Duda JE, Holloway K, Samii A, Horn S, Bronstein JM, Stoner G, et al. (2010) Pallidal versus subthalamic deep-brain stimulation for Parkinson's disease. N Engl J Med 362:2077–2091. CrossRef Medline

Galati S, Mazzone P, Fedele E, Pisani A, Peppe A, Pierantozzi M, Brusa L, Tropepi D, Moschella V, Raiteri M, Stanzione P, Bernardi G, Stefani A (2006) Biochemical and electrophysiological changes of substantia nigra pars reticulata driven by subthalamic stimulation in patients with Parkinson's disease. Eur J Neurosci 23:2923–2928. CrossRef Medline

Gubellini P, Salin P, Kerkerian-Le Goff L, Baunez C (2009) Deep brain stimulation in neurological diseases and experimental models: from molecule to complex behavior. Prog Neurobiol 89:79–123. CrossRef Medline

Hammond C, Rouzaire-Dubois B, Féger J, Jackson A, Crossman AR (1983) Anatomical and electrophysiological studies on the reciprocal projections between the subthalamic nucleus and nucleus tegmenti pedunculopontinus in the rat. Neuroscience 9:41–52. CrossRef Medline

Hannon J, Hoyer D (2008) Molecular biology of 5-HT receptors. Behav Brain Res 195:198–213. CrossRef Medline

Hashemi P, Dankoski EC, Wood KM, Ambrose RE, Wightman RM (2011) In vivo electrochemical evidence for simultaneous 5-HT and histamine release in the rat substantia nigra pars reticulata following medial forebrain bundle stimulation. J Neurochem 118:749–759. CrossRef Medline

Hikosaka O, Takikawa Y, Kawagoe R (2000) Role of the basal ganglia in the control of purposive saccadic eye movements. Physiol Rev 80:953–978. Medline

Huot P, Fox SH, Brotchie JM (2011) The serotonergic system in Parkinson's disease. Prog Neurobiol 95:163–212. CrossRef Medline

Jackson A, Crossman AR (1983) Nucleus tegmenti pedunculopontinus: efferent connections with special reference to the basal ganglia, studied in the rat by anterograde and retrograde transport of horseradish peroxidase. Neuroscience 10:725–765. CrossRef Medline

Jacobs BL, Fornal CA (1999) Activity of serotonergic neurons in behaving animals. Neuropsychopharmacology 21[2 Suppl]:9S–15S. CrossRef Medline

Jacobs BL, Martín-Cora FJ, Fornal CA (2002) Activity of medullary serotonergic neurons in freely moving animals. Brain Res Brain Res Rev 40:45–52. CrossRef Medline

Kaneko M, Takahashi T (2004) Presynaptic mechanism underlying cAMP-dependent synaptic potentiation. J Neurosci 24:5202–5208. CrossRef Medline

Kia HK, Miquel MC, Brisorgueil MJ, Daval G, Riad M, El Mestikawy S, Hamon M, Vergé D (1996) Immunocytochemical localization of serotonin1A receptors in the rat central nervous system. J Comp Neurol 365:289–305. CrossRef Medline

Kish SJ, Tong J, Hornykiewicz O, Rajput A, Chang LJ, Guttman M, Furukawa Y (2008) Preferential loss of serotonin markers in caudate versus putamen in Parkinson's disease. Brain 131:120–131. Medline

Kita H, Kitai ST (1987) Efferent projections of the subthalamic nucleus in the rat: light and electron microscopic analysis with the PHA-L method. J Comp Neurol 260:435–452. CrossRef Medline

Laurent A, Goaillard JM, Cases O, Lebrand C, Gaspar P, Ropert N (2002) Activity-dependent presynaptic effect of serotonin1B receptors on the somatosensory thalamocortical transmission in neonatal mice. J Neurosci 22:886–900. Medline

Li YW, Bayliss DA (1998) Presynaptic inhibition by 5-HT1B receptors of glutamatergic synaptic inputs onto serotonergic caudal raphe neurones in rat. J Physiol 510:121–134. CrossRef Medline

Lozano AM, Snyder BJ, Hamani C, Hutchison WD, Dostrovsky JO (2010) Basal ganglia physiology and deep brain stimulation. Mov Disord 25[Suppl 1]:S71–S75. CrossRef Medline

Maltête D, Jodoin N, Karachi C, Houeto JL, Navarro S, Cornu P, Agid Y, Welter ML (2007) Subthalamic stimulation and neuronal activity in the substantia nigra in Parkinson's disease. J Neurophysiol 97:4017–4022. CrossRef Medline

Maroteaux L, Saudou F, Amlaiky N, Boschert U, Plassat JL, Hen R (1992) Mouse 5HT1B serotonin receptor: cloning, functional expression, and localization in motor control centers. Proc Natl Acad Sci U S A 89:3020–3024. CrossRef Medline

Martinez-Gonzalez C, Bolam JP, Mena-Segovia J (2011) Topographical organization of the pedunculopontine nucleus. Front Neuroanat 5:22. Medline

Millan MJ, Marin P, Bockaert J, Mannoury la Cour C (2008) Signaling at G-protein-coupled serotonin receptors: recent advances and future research directions. Trends Pharmacol Sci 29:454–464. CrossRef Medline

Mizutani H, Hori T, Takahashi T (2006) 5-HT_{1B} receptor-mediated presynaptic inhibition at the calyx of Held of immature rats. Eur J Neurosci 24:1946–1954. CrossRef Medline

Morikawa H, Manzoni OJ, Crabbe JC, Williams JT (2000) Regulation of central synaptic transmission by 5-HT1B auto- and heteroreceptors. Mol Pharmacol 58:1271–1278. Medline

Moukhles H, Bosler O, Bolam JP, Vallée A, Umbriaco D, Geffard M, Doucet G (1997) Quantitative and morphometric data indicate precise cellular interactions between serotonin terminals and postsynaptic targets in rat substantia nigra. Neuroscience 76:1159–1171. CrossRef Medline

Muramatsu M, Lapiz MD, Tanaka E, Grenhoff J (1998) Serotonin inhibits synaptic glutamate currents in rat nucleus accumbens neurons via presynaptic 5-HT1B receptors. Eur J Neurosci 10:2371–2379. CrossRef Medline

Murer MG, Riquelme LA, Tseng KY, Pazo JH (1997) Substantia nigra pars reticulata single unit activity in normal and 6OHDA-lesioned rats: effects of intrastriatal apomorphine and subthalamic lesions. Synapse 27:278–293. CrossRef Medline

Obeso JA, Marin C, Rodriguez-Oroz C, Blesa J, Benitez-Temiño B, Mena-Segovia J, Rodríguez M, Olanow CW (2008) The basal ganglia in Parkinson's disease: current concepts and unexplained observations. Ann Neurol 64[Suppl 2]:S30–S46. Medline

Parent A, Hazrati LN (1995) Functional anatomy of the basal ganglia. II. The place of subthalamic nucleus and external pallidum in basal ganglia circuitry. Brain Res Brain Res Rev 20:128–154. CrossRef Medline

Parent M, Parent A (2007) The microcircuitry of primate subthalamic nucleus. Parkinsonism Relat Disord 13[Suppl 3]:S292–S295. CrossRef Medline

Parent M, Wallman MJ, Descarries L (2010) Distribution and ultrastructural features of the serotonin innervation in rat and squirrel monkey subthalamic nucleus. Eur J Neurosci 31:1233–1242. CrossRef Medline

Parent M, Wallman MJ, Gagnon D, Parent A (2011) Serotonin innervation of basal ganglia in monkeys and humans. J Chem Neuroanat 41:256–265. CrossRef Medline

Perlmutter JS, Mink JW (2006) Deep brain stimulation. Annu Rev Neurosci 29:229–257. CrossRef Medline

Pickard GE, Smith BN, Belenky M, Rea MA, Dudek FE, Sollars PJ (1999) 5-HT1B receptor-mediated presynaptic inhibition of retinal input to the suprachiasmatic nucleus. J Neurosci 19:4034–4045. Medline

Pompeiano M, Palacios JM, Mengod G (1994) Distribution of the serotonin 5-HT2 receptor family mRNAs: comparison between 5-HT2A and 5-HT2C receptors. Brain Res Mol Brain Res 23:163–178. CrossRef Medline

Riad M, Garcia S, Watkins KC, Jodoin N, Doucet E, Langlois X, el Mestikawy S, Hamon M, Descarries L (2000) Somatodendritic localization of

5-HT1A and preterminal axonal localization of 5-HT1B serotonin receptors in adult rat brain. J Comp Neurol 417:181–194. CrossRef Medline

Ryan LJ, Sanders DJ (1993) Subthalamic nucleus lesion regularizes firing patterns in globus pallidus and substantia nigra pars reticulata neurons in rats. Brain Res 626:327–331. CrossRef Medline

Sari Y (2004) Serotonin1B receptors: from protein to physiological function and behavior. Neurosci Biobehav Rev 28:565–582. CrossRef Medline

Sari Y, Miquel MC, Brisorgueil MJ, Ruiz G, Doucet E, Hamon M, Vergé D (1999) Cellular and subcellular localization of 5-hydroxytryptamine1B receptors in the rat central nervous system: immunocytochemical, autoradiographic and lesion studies. Neuroscience 88:899–915. CrossRef Medline

Sato F, Parent M, Levesque M, Parent A (2000) Axonal branching pattern of neurons of the subthalamic nucleus in primates. J Comp Neurol 424:142–152. CrossRef Medline

Shen KZ, Johnson SW (2006) Subthalamic stimulation evokes complex EPSCs in the rat substantia nigra pars reticulata in vitro. J Physiol 573:697–709. CrossRef Medline

Shen KZ, Johnson SW (2012) Regulation of polysynaptic subthalamonigral transmission by D2, D3 and D4 dopamine receptors in rat brain slices. J Physiol 590:2273–2284. Medline

Shen KZ, Kozell LB, Johnson SW (2007) Multiple conductances are modulated by 5-HT receptor subtypes in rat subthalamic nucleus neurons. Neuroscience 148:996–1003. CrossRef Medline

Singer JH, Bellingham MC, Berger AJ (1996) Presynaptic inhibition of glutamatergic synaptic transmission to rat motoneurons by serotonin. J Neurophysiol 76:799–807. Medline

Smith Y, Parent A (1988) Neurons of the subthalamic nucleus in primates display glutamate but not GABA immunoreactivity. Brain Res 453:353–356. CrossRef Medline

Smith Y, Hazrati LN, Parent A (1990) Efferent projections of the subthalamic nucleus in the squirrel monkey as studied by the PHA-L anterograde tracing method. J Comp Neurol 294:306–323. CrossRef Medline

Stanford IM, Lacey MG (1996) Differential actions of serotonin, mediated by 5-HT1B and 5-HT2C receptors, on GABA-mediated synaptic input to rat substantia nigra pars reticulata neurons *in vitro*. J Neurosci 16:7566–7573. Medline

Steigerwald F, Pötter M, Herzog J, Pinsker M, Kopper F, Mehdorn H, Deuschl G, Volkmann J (2008) Neuronal activity of the human subthalamic nucleus in the parkinsonian and nonparkinsonian state. J Neurophysiol 100:2515–2524. CrossRef Medline

Steinbusch HW (1981) Distribution of serotonin-immunoreactivity in the central nervous system of the rat-cell bodies and terminals. Neuroscience 6:557–618. CrossRef Medline

Sudhof TC (2004) The synaptic vesicle cycle. Annu Rev Neurosci 27:509–547. CrossRef Medline

Thomson AM (2000) Molecular frequency filters at central synapses. Prog Neurobiol 62:159–196. CrossRef Medline

Tseng KY, Riquelme LA, Belforte JE, Pazo JH, Murer MG (2000) Substantia nigra pars reticulata units in 6-hydroxydopamine-lesioned rats: responses to striatal D2 dopamine receptor stimulation and subthalamic lesions. Eur J Neurosci 12:247–256. CrossRef Medline

Voigt MM, Laurie DJ, Seeburg PH, Bach A (1991) Molecular cloning and characterization of a rat brain cDNA encoding a 5-hydroxytryptamine1B receptor. EMBO J 10:4017–4023. Medline

Wallmichrath I, Szabo B (2002) Cannabinoids inhibit striatonigral GABAergic neurotransmission in the mouse. Neuroscience 113:671–682. CrossRef Medline

Wichmann T, Dostrovsky JO (2011) Pathological basal ganglia activity in movement disorders. Neuroscience 198:232–244. CrossRef Medline

Wichmann T, DeLong MR, Guridi J, Obeso JA (2011) Milestones in research on the pathophysiology of Parkinson's disease. Mov Disord 26:1032–1041. CrossRef Medline

Wilson CJ, Bevan MD (2011) Intrinsic dynamics and synaptic inputs control the activity patterns of subthalamic nucleus neurons in health and in Parkinson's disease. Neuroscience 198:54–68. CrossRef Medline

Xiang Z, Wang L, Kitai ST (2005) Modulation of spontaneous firing in rat subthalamic neurons by 5-HT receptor subtypes. J Neurophysiol 93:1145–1157. Medline

Yao L, Sakaba T (2010) cAMP modulates intracellular $Ca2^+$ sensitivity of fast-releasing synaptic vesicles at the calyx of Held synapse. J Neurophysiol 104:3250–3260. CrossRef Medline

Zhou FM, Lee CR (2011) Intrinsic and integrative properties of substantia nigra pars reticulata neurons. Neuroscience 198:69–94. CrossRef Medline

Zhou FW, Xu JJ, Zhao Y, LeDoux MS, Zhou FM (2006) Opposite functions of histamine H1 and H2 receptors and H3 receptor in substantia nigra pars reticulata. J Neurophysiol 96:1581–1591. CrossRef Medline

Zhou FW, Matta SG, Zhou FM (2008) Constitutively active TRPC3 channels regulate basal ganglia output neurons. J Neurosci 28:473–482. CrossRef Medline

Zucker RS, Regehr WG (2002) Short-term synaptic plasticity. Annu Rev Physiol 64:355–405. CrossRef Medline